Energy redistribution in railway transition zones by geometric optimisation of a novel transition structure

Jain, A.; Metrikine, A. V.; van Dalen, K. N.

DOI
10.1016/j.trgeo.2024.101383

Publication date
2024

Document Version
Final published version

Published in
Transportation Geotechnics

Transportation Geotechnics 49 (2024) 101383

Contents lists available at ScienceDirect

Transportation Geotechnics

journal homepage: www.elsevier.com/locate/trgeo

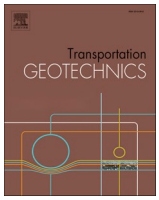

Original Article

Energy redistribution in railway transition zones by geometric optimisation of a novel transition structure

A. Jain *, A.V. Metrikine, K.N. van Dalen

Faculty of Civil Engineering and Geosciences (CEG), Department of Engineering Structures, TU Delft, Stevinweg 1, Delft 2628 CN, the Netherlands

ARTICLE INFO

Keywords:
Railway transition zones
Geometric optimisation
Transition structure
SHIELD
Strain energy distribution

ABSTRACT

Railway transition zones are critical regions in railway infrastructure that are subjected to excessive operation-driven degradation due to energy concentration within these zones. This work presents a heuristic approach to optimise the geometry of the transition structure and investigate its influence on the strain energy distribution in the railway transition zones (RTZs), with a specific focus on embankment-bridge transitions equipped with a newly proposed 'Safe Hull-Inspired Energy Limiting Design (SHIELD)' transition structure. For this purpose, a number of three-dimensional finite element models are used to analyze different geometric profiles of SHIELD in a systematic manner. By altering SHIELD's geometry across longitudinal, transversal, and vertical directions, the influence of the different geometric profiles on the total strain energy distribution across the trackbed layers (ballast, embankment, and subgrade) is studied in terms of spatial and temporal variations. The results establish the contribution of geometry to energy redistribution in all three directions and present an optimum geometry for the type of transition under study. It is found that among all the profiles, the longitudinal geometric profile of SHIELD has the most significant impact on the strain energy distribution, while the transversal profile primarily influences the ballast layer, and the alteration of vertical profiles enhance the local redistribution of strain energy in the vicinity of the transition interface. The preliminary optimisation (heuristic approach) presented in this work provides the starting point for full-scale optimisation to obtain tailored shapes of transition structures such that there is neither a concentration of energy nor an obstruction in the flow of energy in RTZs.

Introduction

Railway transition zones (RTZs), where track configurations change from one type of foundation to another (e.g., from a bridge onto an embankment or from slab track to ballasted track), represent critical sections in railway networks. Several studies [1–3] highlight the vulnerability of RTZs to geometry and material degradation leading to high maintenance costs [4]. In [5], a detailed overview of the problem in RTZs is presented highlighting the main causes behind the accelerated deterioration of track material and geometry in RTZs. Another study [6] provides a comprehensive review of various mitigation measures adopted to deal with the amplified degradation of RTZs. The zones are typically characterized by abrupt changes in track stiffness [7] and differential settlement [8–10] and are often subjected to dynamic amplifications. Over the years, these amplifications have been studied vastly in terms of kinematic responses or stresses in the track components such as rail, sleepers and trackbed layers (ballast, embankment, subgrade). However, in a recent study [11], the strain energy is proposed to be the most comprehensive quantity (as it includes both stress and strain) to study the operation-driven response amplifications in railway transition zones. Moreover, the total strain energy includes not only the distortional component (related to Von-Mises stress) but also the volumetric component of the strain energy. The study has concluded that "minimizing the magnitude of total strain energy (as the non-recoverable part of the strain energy contributes to the damage in material) will imply lesser permanent deformation and hence reduced operation-induced degradation, and the total strain energy being as uniform as possible along the longitudinal direction (i.e., without an abrupt increase or decrease) will mitigate non-uniform (operation-induced) degradation". The study performed to formulate this design criterion clearly shows the amplification of strain energy in typical RTZs. However, this investigation was performed using a 2 dimensional (2-D) plane-strain finite element model. Even though some studies have shown that the amplified degradation in RTZs can be studied to some extent using equivalent 2-D models [12–15], the influence of the geometry in the transverse direction on the strain energy distribution is

* Corresponding author.
E-mail address: A.jain-1@tudelft.nl (A. Jain).

https://doi.org/10.1016/j.trgeo.2024.101383
Received 14 May 2024; Received in revised form 29 August 2024; Accepted 20 September 2024
Available online 30 September 2024

unknown. The investigation of strain energy variations in the trackbed layers using a 3-D model [16–19] is lacking in the literature.

There have been numerous attempts at designing an effective intervention to mitigate the effects of dynamic amplifications in railway transition zones. Some of the most commonly used interventions are transition structures such as approach slabs [20–23], transition wedges [24–27], auxiliary rails [28,29] closely spaced sleepers [30], undersleeper pads [31] and others [3,32,33]. Based on the recently proposed energy-based criterion mentioned above [11], it is shown in [34,30] that most of these mitigation measures either have no effect on reducing energy amplifications close to the transition interface or may even amplify the strain energy elsewhere in the system. A novel Safe Hull-Inspired Energy Limiting Design (SHIELD) of a transition structure is adopted in [34] using the design principle of guiding energy away from the upper trackbed layers such that there is neither a concentration of energy in any part of the system nor an obstruction in the flow of energy in any of the trackbed layers. Fig. 1 shows energy concentration in the upper trackbed layers due to geometry [34] and energy obstruction in the transition zone compared to the open tracks for an embankment-bridge transition discussed in Section Models. SHIELD as a name reflects that the transition structure design is 'safe' (as the transition structure safeguards the track from excessive degradation), 'hull-inspired' (as the geometry of the transition structure is inspired by the shape of a hull) and 'energy-limiting' (as the key phenomena governing design are based on limiting energy around the transition zones). However, these studies are based on a 2-D model of SHIELD. There is a need for comprehensive research targeting the effects of the various geometric profiles of this newly proposed design. The geometric profiles in longitudinal, transverse and vertical directions can play a pivotal role in the distribution of the strain energy in RTZs. A deeper understanding of this interplay between geometry and energy distributions can offer transformative insights into optimizing design, ensuring robustness, and extending the lifespan of RTZs. In this work, the influence of geometry on energy distributions is investigated, and the influence of energy distributions on geometry (permanent deformations in the vertical direction) is demonstrated in [11].

The role of geometry in guiding energy is paramount, especially in systems like RTZs where obstruction-free flow [35–37] and uniform distribution of energy are sought [38]. Geometry serves as a fundamental determinant in the path and characteristics of energy flow within a system. The role of geometry in energy distribution can be explained in terms of the following items:

- **Guiding energy using optimal pathways:** The shape and configuration of a structure can significantly influence the propagation of energy. For instance, certain geometric designs can ensure that wave energy gets distributed uniformly rather than concentrating in specific areas, preventing "hotspots" or areas of concentrated energy. Geometry can be utilized to design optimal pathways such that the energy flow within railway transition zones can be guided to shield the most degradation-prone components from energy concentration or obstruction, thus preventing localized zones of high energy.
- **Scattering and reflection:** The geometry of a specific surface can determine how energy is reflected or scattered. Curved or angled surfaces, for instance, might scatter energy more effectively than flat ones, preventing energy concentration.
- **Mitigating stress concentrations:** Sharp corners or sudden changes in cross-section can lead to stress concentrations. By optimizing geometry, these concentrations can be minimized, ensuring a more uniform distribution of energy.

In summary, geometry serves as a blueprint for energy flow. By understanding the interplay between geometry and energy, designers and scientists can create systems that channel and distribute energy in desired and efficient ways.

This paper presents a detailed investigation of the influence exerted by geometry on the strain energy distributions induced by moving loads in RTZs. Firstly, a 3-D model of a standard embankment-bridge transition without any transition structure is studied to evaluate the distribution of total strain energy in the trackbed layers in the proximity of the transition interface and far from it. Secondly, the influence of different geometric profiles of SHIELD in longitudinal, transverse and vertical

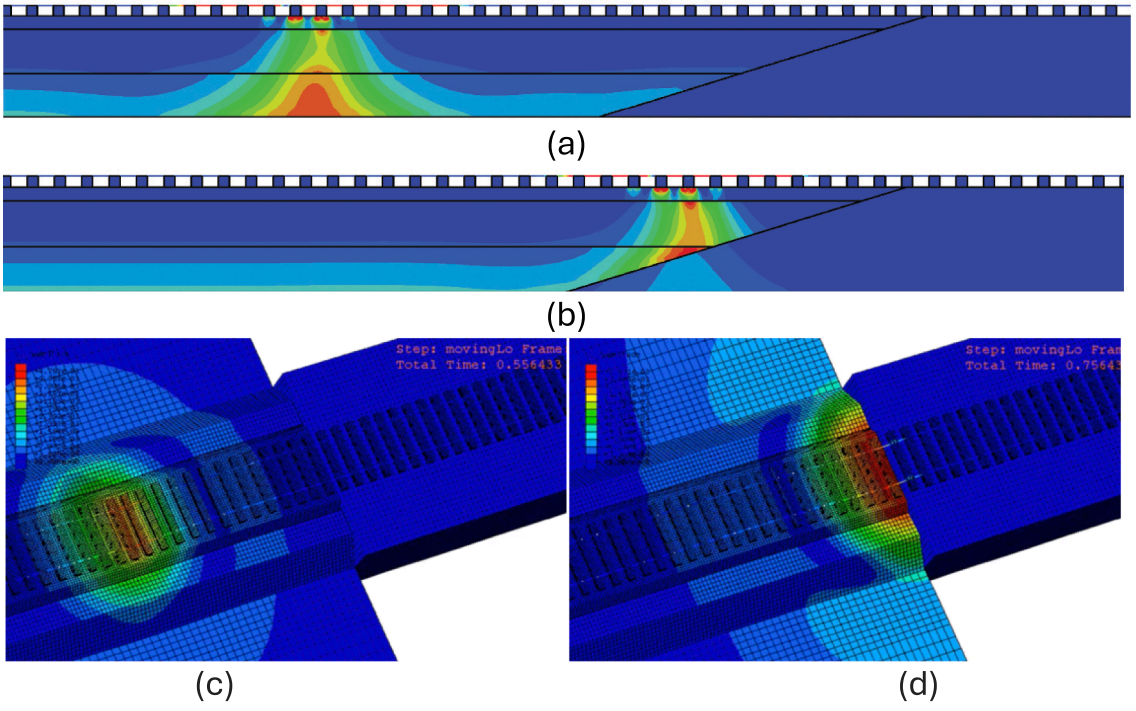

Fig. 1. (a) 2-dimensional model showing energy flow in the open track in the longitudinal direction [34] and (b) energy concentration in upper trackbed layers [34] compared to open tracks due to geometry. (c) 3-dimensional model showing energy flow in the open track and (d) energy obstruction in the .transition zone.

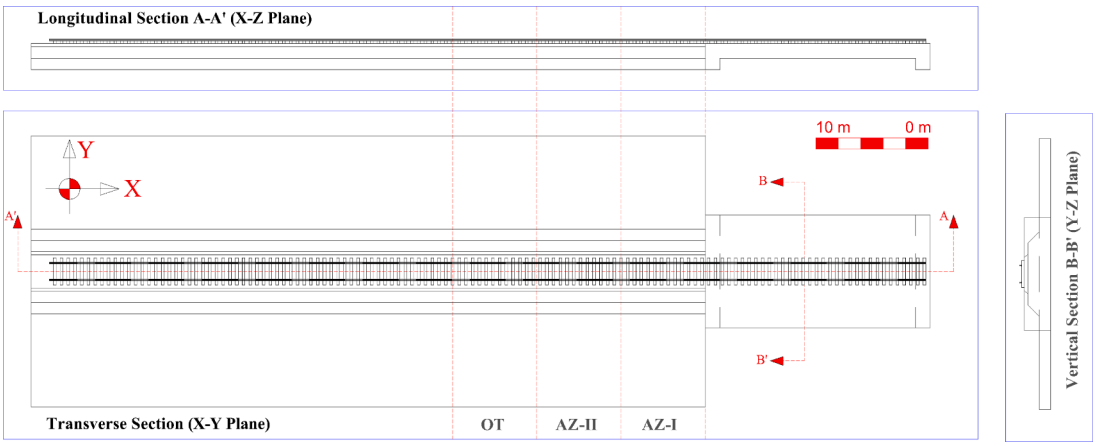

Fig. 2. Cross-section details of a standard embankment-bridge transition used to generate a 3-D numerical model.

directions on the strain energy distributions is studied using a number of 3-D finite element models (discussed in detail in Section Models). Lastly, based on the results (in Section Results and discussion) obtained for the above-mentioned cases, this paper presents an optimised geometry of the transition structure using a heuristic approach for energy redistribution in RTZs. It is to be noted that apart from the geometric profiles, all other parameters like mechanical properties of the materials, train speed and direction, type of transition etc., are kept constant in this work. The influence of mechanical properties of materials has been investigated in [39] and the influence of other parameters using more detailed models will be investigated in future works.

Models

In this paper, the dynamic behaviour of railway transition zones is studied for a standard embankment-bridge transition with and without a transition structure. For this purpose, a number of models are generated and will be discussed in detail in this section. It is to be noted that all materials used in this work are linear elastic as a correlation was demonstrated in [11] between strain energy amplifications and permanent deformations. The models studied in this work can be broadly classified into two categories as follows:

- **Standard embankment-bridge transition zone:** A three-dimensional (3-D) finite element model was developed using ABAQUS [40] to represent an embankment-bridge railway transition zone to study the influence of the geometry in all directions on the distribution of total strain energy in the trackbed layers. This model is referred to as the "base model" in this work. The improved behaviour of RTZs with the new transition structure (SHIELD; see category 2 below) is shown in comparison to this base model.
- **Embankment-bridge transition zone incorporating the "Safe Hull Inspired Energy Limiting Design" (SHIELD) transition structure:** The influence of longitudinal, transverse and vertical geometric profiles of SHIELD on the distribution of strain energy in each trackbed layer is studied using a variety of models. The geometric profiles shown in Figs. 3–5 are chosen such that the energy is guided away from the trackbed layers prone to degradation, there is no energy amplification due to adverse effects of reflection and scattering and there are no stress concentrations due to sharp geometric edges (based on discussions in Introduction). Firstly, five longitudinal profiles (see Fig. 3 and Table 1 for details) of SHIELD are studied using two-dimensional plane-strain models. A two-dimensional model is used in this step to avoid the influence of out-of-plane geometry, which is investigated in the subsequent steps. Secondly, the longitudinal profile that shows the most promising dynamic behaviour according to the energy criterion (as discussed in the Introduction) is chosen as a basis for the generation of a 3-D shape of SHIELD with varying transversal cross-sections (see Fig. 4 and Fig. 5 for details). Lastly, the influence of the vertical cross-section (see Fig. 6 and Fig. 7 for details) is investigated using the longitudinal and transverse profiles that show the best performance according to the energy criterion.

Geometric model

Base model

The geometric profiles (longitudinal, transverse, and vertical) of the base model are shown in Fig. 2. In Fig. 2, the longitudinal profile is in the X-Z plane, the transverse profile is in the X-Y plane and the vertical profile belongs to the Y-Z plane. The total length of the base model in the longitudinal direction is 80 m which is comprised of 60 m of ballasted track (soft side) and 20 m of ballast-less track (concrete bridge). The ballasted track is divided into three zones of 7.5 m each with an additional 22.5 m at the end in order to eliminate the influence of boundaries (extreme left and right) on the results of the zones under study. The first zone (see Fig. 2 for zoning details) close to the transition interface is

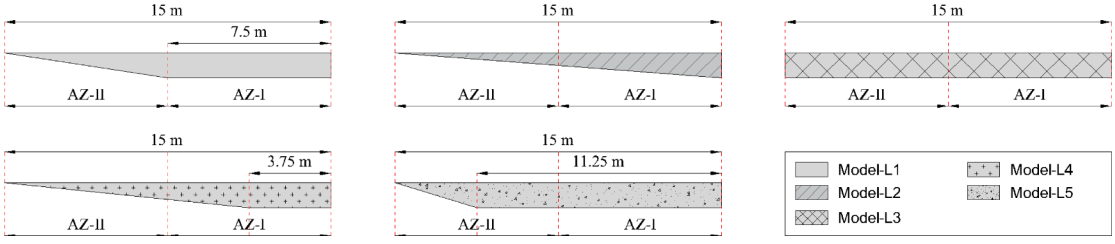

Fig. 3. Longitudinal profiles of SHIELD (models L1 to L5 as shown in the legend).

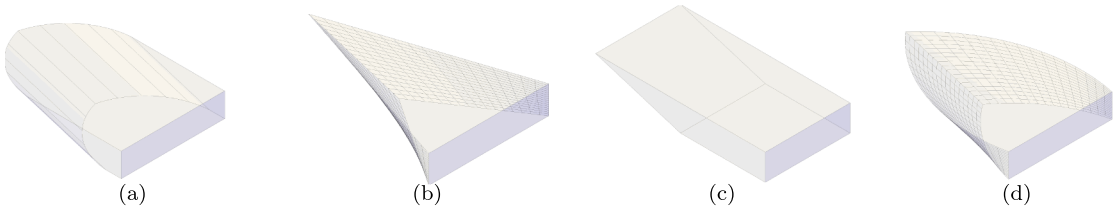

Fig. 4. Three-dimensional (3-D) shapes of SHIELD with different transverse cross-sections for (a) Model-T1, (b) Model-T2, (c) Model-T3, (d) Model-T4.

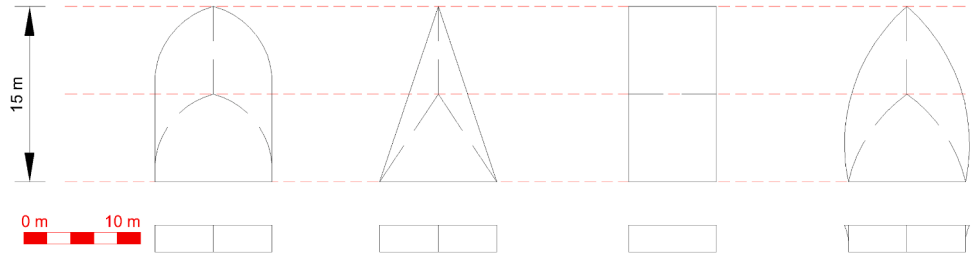

Fig. 5. Transverse and vertical cross-sections of SHIELD for Model-T1, Model-T2, Model-T3, Model-T4 (left to right).

Table 1
Details of Longitudinal profiles of SHIELD studied in this paper.

Longitudinal Profiles	L_{top}	L_{bottom}	Schematic (models L1-L5)
Model-L1	L	$L/2$	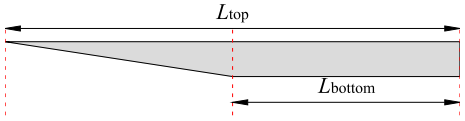
Model-L2	L	null	
Model-L3	L	L	
Model-L4	L	$L/4$	
Model-L5	L	$3L/4$	

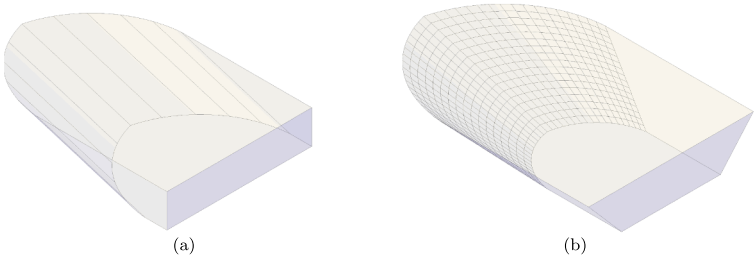

Fig. 6. Three dimensional (3-D) shapes of SHIELD with different vertical cross-sections for (a) Model-V1, (b) Model-V2.

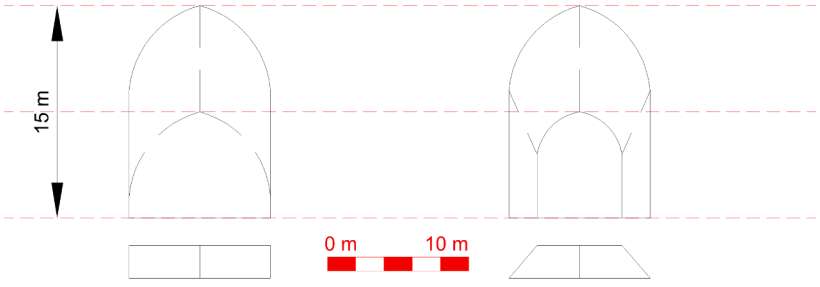

Fig. 7. Transverse and vertical cross-sections of SHIELD for Model-V1 and Model-V2 (left to right).

referred to as ”Approach Zone - I (AZ-I)” which is the most influenced zone by transition effects. The last zone under study is referred to as ”Open Track (OT)” as it is largely uninfluenced by transition effects. The second zone in between AZ-I and OT is referred to as ”Approach Zone–II (AZ-II)” which might or might not be affected by transition effects. The geometric model mainly consists of the following track components:

- Rail with profile 54E1 (UIC54) according to European Standard EN 13674–1
- Rail-pads
- Sleepers
- Trackbed layers: Ballast, Embankment, Natural terrain or subgrade
- Concrete bridge

The sleeper spacing adopted is 0.6 m and the first sleeper next to the transition is located at 0.3 m from the transition interface.

SHIELD

The base model described above was modified by inserting various geometric shapes of SHIELD between the ballasted track and the concrete bridge. The different geometric profiles of SHIELD investigated in this paper are described in detail below.

Longitudinal profiles of SHIELD The longitudinal profile of SHIELD is a trapezoidal-shaped geometry with a major base (top) of length 'L_{top}' and a minor base (bottom) of length 'L_{bottom}' as shown in the schematic in Table 1. Five different longitudinal profiles (see Fig. 3) are studied and listed below.

It is to be noted that models L1-L5 are studied to investigate the influence of the ratio of L_{top} to L_{bottom} of the transition structure. However, the design length 'L' mentioned in Table 1 will depend on several factors such as vehicle characteristics, material properties of the surrounding/environment, type of transition zone, etc. However, as the aim of this work is to demonstrate the influence of the geometric parameters of the longitudinal profile of the SHIELD on the strain energy distribution in the trackbed layers, all other parameters are kept constant. For a particular set of the above-mentioned factors considered in this work, $L = 15$ m was found to be the optimum length to mitigate the transition effects.

Transverse profiles of SHIELD The transverse profiles of SHIELD presented in this paragraph are based on the principle of guiding energy away from the trackbed layer (as discussed in the Introduction) in the transverse direction. As shown in Fig. 4 and Fig. 5, two extreme profiles of rectangular (model-T3) and triangular (model-T2) shaped geometry are considered. In addition to this, model-T4 (lanceolate-shaped) is a modification of model-T2 exhibiting curved edges around the apex and model-T1 (a combination of model-T3 and model-T4) has a rectangular-shaped bottom and lanceolate-shaped top. The transverse profiles of all the models are such that the volume of all the models is comparable, the vertical cross-section at the transition interface is rectangular and the longitudinal cross-section is similar to that of model-L1.

Vertical profiles of SHIELD Two vertical profiles of SHIELD are investigated to see the influence of tapering in the vertical plane on the energy distribution in the trackbed layers. The vertical profiles model-V1 (trapezoidal-shaped) and model-V2 (rectangular-shaped) are studied (see Fig. 6 and Fig. 7). It is to be noted that model-T1 was chosen to study the variation of the vertical-plane geometry of SHIELD as it shows the most favourable distribution of strain energy as per the criterion, as discussed later (in Section Outputs).

The total length of all the models described above is the same as the base model. However, the division of the zones is different in order to study the dynamic behaviour of the transition structure in detail. Each zone (AZ-I, AZ-II, AZ-III) is 7.5 m for all the above-mentioned cases with SHIELD. The open track behaviour is expected to be the same as that predicted by the base model. The first zone close to the transition interface between the bridge and transition structure is referred to as "Approach Zone-III (AZ-III)", and the last zone next to the interface between the ballasted track and transition structure is referred to as "Approach Zone–I (AZ-I)". The zone in between AZ-I and AZ-III is referred to as "Approach Zone–II (AZ-II)". All the track components remain the same as the base model, only the transition structure (SHIELD) is added. Fig. 8 shows the zones of study for one of the models (model-V1) with SHIELD.

Numerical model

Several 3-D Finite Element (FE) models were created using ABAQUS, by modifying the base model (Fig. 9) using geometrical details described in Section Geometric model. To include realistic energy dissipation in the models, Rayleigh damping for materials was defined using parameters listed in Table 2 according to [39]. The dimensions (longitudinal and vertical direction) of the model were chosen to eliminate the influence of the wave reflections from the boundaries (extreme right, left and bottom of the system) on the results of the zones under study. The depth of the subgrade was limited to restrict the vertical displacements to maintain a reasonable value based on literature [41]. In addition to this, the cumulative depth of the layers under the sleepers is maintained such that the dynamic stresses at the bottom of the subgrade are less than 3% (this value was suggested to be less than 10% in [12] so as to eliminate artificial boundary effects) of their values at the bottom of the sleepers. Moreover, the vertical rail displacements and stress in the ballast layer were verified with the data presented in [42,43] for a transition zone similar to the one under study, and values obtained from the base model (rail displacement $= 1.47$ mm) are comparable to the ones mentioned in the literature (rail displacement $= 1.39$ mm approx.) [42].

The following subsections describe the details regarding the FE models used in this paper in terms of mesh properties, mechanical properties of materials, interactions between the track components, loads and boundary conditions. A static step was performed to obtain the initial stress state of the model under self-weight, followed by a dynamic analysis (full Newton–Raphson method) for 2.5 s with a time step of 0.005 s. The loads that have been considered are the gravity load for the static analysis and one moving axle load of 90 kN with a velocity of 100 km/h for the dynamic analysis. It is to be noted that the simplest loading conditions have been adopted in this work as the main objective is to

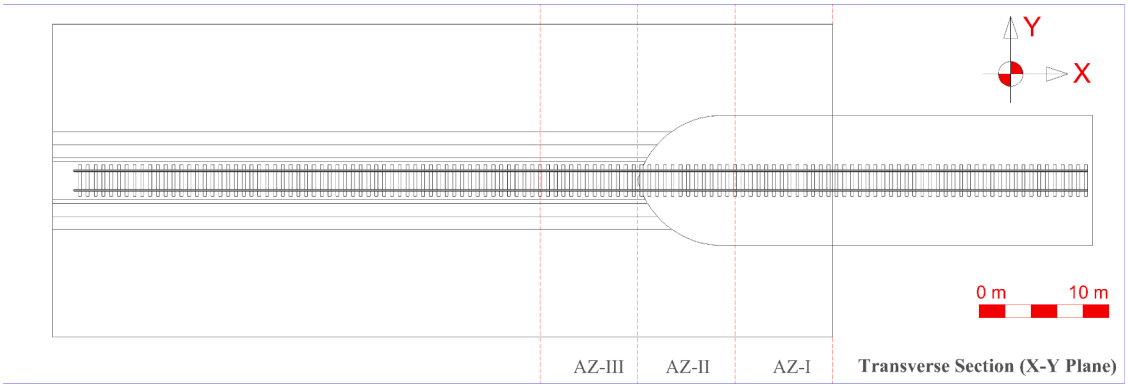

Fig. 8. Transverse Cross-section of the model-V1 showing the zones (AZ-I, AZ-II, AZ-III) under study.

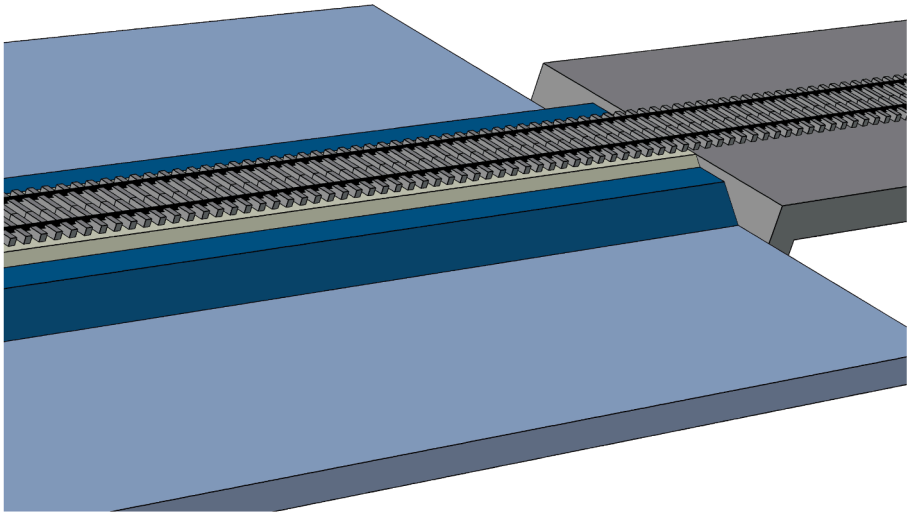

Fig. 9. The 3-D finite element model (mesh elements are deactivated for better visualization) of a standard embankment-bridge transition (base model) generated using ABAQUS.

Table 2
Mechanical properties of the track components.

Material	Elasticity Modulus E [N/m^2]	Density ρ [kg/m^3]	Poisson's Ratio ν	Rayleigh damping α	β
Steel (rail)	21×10^{10}	7850	0.3	–	–
Concrete (sleepers)	3.5×10^{10}	2400	0.15	–	–
Ballast	1.5×10^{8}	1560	0.2	0.0439	0.0091
Sand (embankment)	8×10^{7}	1810	0.3	8.52	0.0004
Clay (subgrade)	2.55×10^{7}	1730	0.3	8.52	0.0029
SHIELD	3.6×10^{8}	1900	0.2	0.0439	0.0091

investigate the influence of geometry on the energy distributions, capturing the main mechanisms governing the dynamic amplifications in RTZs in the cleanest possible manner. The load moving in the direction from the soft side to the stiff side of the transition was simulated using the DLOAD subroutine in ABAQUS [44].

Material

The materials used for all track components in the models described in previous sections are characterised by elastic properties (Young's modulus, Poisson's ratio), densities and Rayleigh damping factors [45,46]. A detailed analysis of the influence of material properties was performed in [39] and suggested stiffness ratios were used for optimal performance of SHIELD in this work. The mechanical properties of all the track components and the transition structure (SHIELD) are chosen as tabulated in Table 2 for this study.

Interface and boundary conditions

The infinite elements (CIN3D4R) are used on the vertical boundaries at extreme left and right to minimize reflections due to artificial boundaries. The interface conditions used in the models are defined below:

- Rail-sleeper: Rail was connected to the sleepers via rail-pads using vertical springs with stiffness ($k = 1.2$ x 10^8 N/m) and dashpots with coefficient ($c = 5 \times 10^4$ N-s/m).
- Sleeper-ballast, ballast-embankment, and embankment-subgrade interfaces: surface-to-surface tie constraint was used for defining the conditions at these three interfaces.
- All vertical interfaces: a hard contact linear penalty method was used to define the normal behaviour and Coulomb's friction law was adopted to define the tangential behaviour with a frictional coefficient equal to 0.5. (details can be found in [40])

Mesh

In all the 3-D models, sleeper, ballast, embankment, subgrade, transition structure and bridge were discretized [40] using four-node tetrahedral elements (C3D4) the eight-node brick elements (C3D8). The rail was discretized using two-node linear beam elements of type B21 to form a very regular mesh. An initial mesh sensitivity analysis was performed for each of the models to ensure that there is no dependence of the results on the mesh size or quality.

Outputs

The main outputs from the models studied in this paper are time histories of the total strain energy (only dynamic) in each of the zones under study for the layers of ballast, embankment and subgrade. In Abaqus [44], "ALLSE" provides a time history of the total strain energy within a considered volume (each zone for each trackbed layer). These outputs are compared for the different geometric profiles (Section Geometric model for details) of SHIELD and the base model under study.

The strain energy magnitude on the concrete structure (stiff side) is negligible (approximately 300 times smaller) compared to the ballasted tracks (soft side) as shown in [11] and a direct correlation was demonstrated between strain energy and permanent deformations. This implies a large difference in the permanent deformations on the soft and stiff side of the system. In order to avoid an abrupt drop of strain energy from the soft to the stiff side of the system, SHIELD was proposed [34,39] to facilitate a gradual decrease in strain energy magnitudes (and thus in permanent deformation). In terms of magnitude (spatially), the ratio of maximum strain energy in consecutive zones shown in Fig. 10 is desired to be always less than 1. In the temporal variation of strain

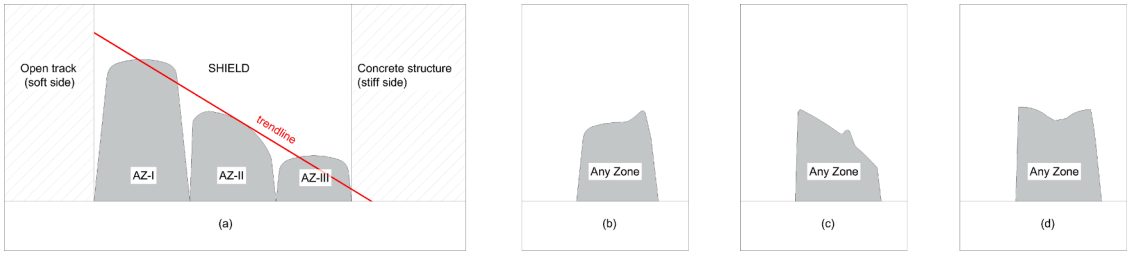

Fig. 10. Schematic showing (a) spatial trend of the strain energy in zones from open track to concrete structure and its temporal trend within one zone: (b, c) abrupt local increase, (d) increase after decreasing trend.

energy, a monotonically decreasing trend is sought. Both of these requirements are directly inferred from the general criterion presented in [11]. The performance of different geometric profiles of SHIELD is assessed in terms of the following evaluation criteria (which directly follow from the design criterion referred to in the Introduction):

- Spatial trend: The variation of strain energy magnitudes from the open track to the concrete structure must demonstrate a gradual "decreasing trend". This implies the strain energy magnitude must gradually decrease from one zone under study to another (from the largest in AZ-I to the lowest in AZ-III)) as shown in the schematic (Fig. 10a).
- Temporal trend: Within each zone, the temporal variation of strain energy must demonstrate "smoothness". This implies that the strain energy curve must not exhibit sharp spikes or drastic changes (increase or decrease) in a short span of time (Fig. 10b,c). In addition to this, within each zone, ideally, the strain energy magnitude must never increase after a decreasing trend is observed at any time moment (see Fig. 10d). This type of local increase might lead to locally amplified degradation (e.g., hanging sleepers). It is to be noted that there is always an entrance effect or initial rise in strain energy magnitude due to the entrance of the deformation field carried by the moving load.

Results and discussion

Base Model

As discussed in the Introduction, the investigation of strain energy variations in track components using a 3-D model is lacking in the literature. Therefore, in this section, the time histories of strain energy (Fig. 11c) for the base case (described in Section Models) obtained using a 2-D model and a 3-D model are compared for the layers of ballast, embankment and subgrade in the zones under study (OT, AZ-I and AZ-II). It is observed that the plane-strain assumption of the 2-D model leads to an overestimation of the strain energy (given the same loading conditions) in the embankment and subgrade and shows a higher amplification of strain energy in the proximity of the transition interface in the ballast layer compared to that predicted by the 3-D model. The overestimation of responses can also be seen in a comparison of displacements (see Fig. 12) obtained for 4 points (on rail, top of ballast, embankment and subgrade under rail) in the open track. The track components in the 2-D model deform much more than in the 3-D model. Even though the 2-D model captures the trends of strain energies in all the layers and zones under study, designers must rely on 3-D models for precise calculations.

In Fig. 12, for the layers of ballast and embankment, it can be clearly seen that there is an amplification of strain energy in the AZ-II with respect to the OT in the proximity of the transition interface. Moreover, even though there is no strain energy amplification in AZ-II with respect to OT in the subgrade layer, the strain energy is non-zero (unlike other layers) even after the load has crossed the transition interface. In order to minimise the transition effects, it is necessary to minimise the strain energy amplifications in the affected trackbed layers. An effective intervention must ensure no amplification in strain energy in any of the trackbed layers under study in the proximity of the transition interface between the ballasted track and transition structure and between the transition structure and the concrete bridge. The following section will demonstrate the influence of geometric profiles on energy redistribution in the railway transition zone.

Longitudinal profiles of SHIELD

Ballast: Fig. 13 shows a comparison of the time histories of strain energy in the ballast layer for the zones AZ-I, AZ-II and AZ-III for models L1-L5. It can be clearly seen that in AZ-I, model-L3 and model-L5 exhibit an amplification of strain energy at the time moment right before the load exits AZ-I. This is similar to AZ-II of the base model (Fig. 11) as expected due to the rectangular shape of the transition structure in model-L3 and the very steep slope of the inclined interface for model-L5. In summary, models L3 and L5 are not suitable geometric profiles as they show strain energy amplification similar to the base model with the only difference of location. In the base model, this amplification is observed at the interface of ballast and the concrete structure, whereas, in models L3 and L5, the strain energy amplification is observed at the interface of ballast and SHIELD. Therefore, the study can be narrowed down to

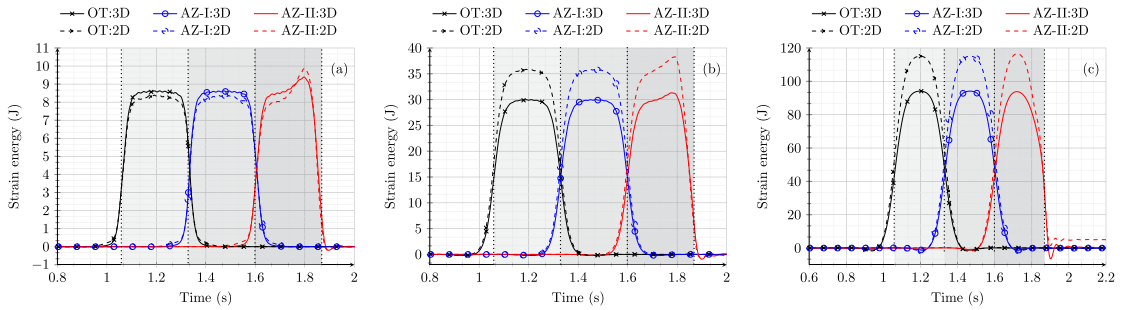

Fig. 11. Time history of the strain energy obtained from the base model for the layers of (a) ballast, (b) embankment and (c) subgrade in all the zones under study (OT, AZ-I, AZ-II). The dotted lines mark the time moments at which the load enters and exits each zone.

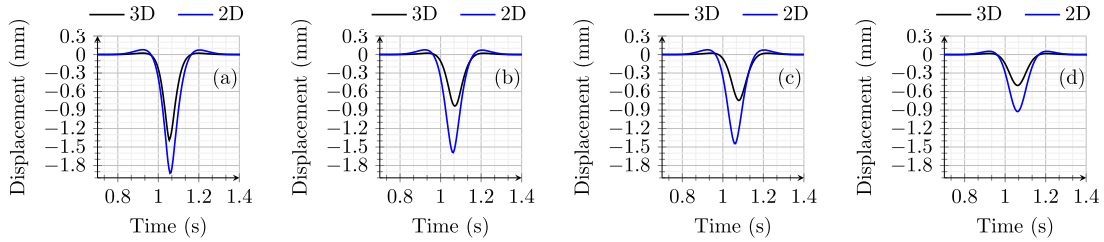

Fig. 12. Time history of the displacements obtained from the base model for (a) rail, top of (b) ballast (c) embankment and (d)subgrade layers.

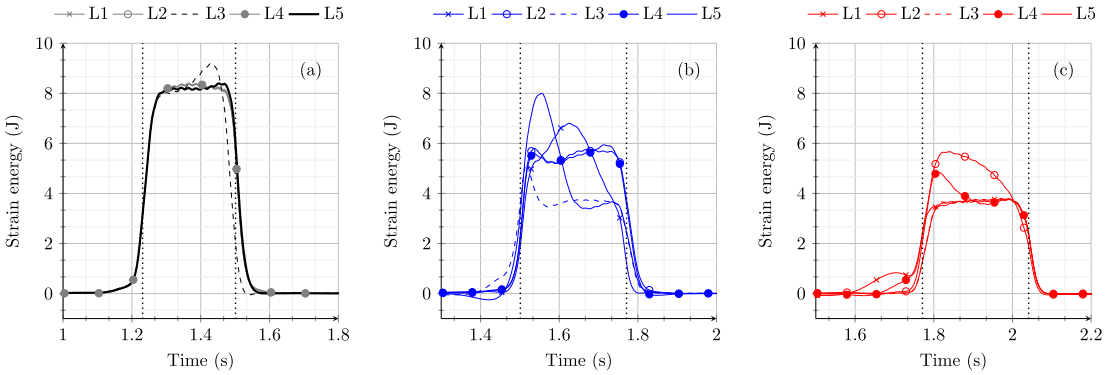

Fig. 13. Time history of strain energy for different longitudinal profiles under study in the layer of ballast for (a) AZ-I, (b) AZ-II and (c) AZ-III. The dotted lines mark the time moments at which the load enters and exits each zone.

models L1, L2 and L4. In AZ-II, all these models show similar behaviour in terms of the magnitude of strain energy, but both a spatial (from one zone to the other as the load moves from AZ-I to AZ-III) and a temporal (within each zone) decreasing trend (as discussed in Section Outputs) can be seen only in model-L1. models L2 and L4 show unfavourable behaviour as they demonstrate a decrease after the time moment at which the load enters AZ-II (similar to Fig. 11) and an increase right before the load exits this zone. In AZ-III, none of the models show an abrupt increase in strain energy (temporal) but the spatially decreasing trend (from AZ-II to AZ-III) is observed only for model-L1. models L2 and L4 show a higher magnitude of strain energy compared to model L1 in AZ-III.

Embankment: Fig. 14 shows a comparison of the time history of strain energy in the embankment layer for zones AZ-I, AZ-II and AZ-III for models L1-L5. Similar to the ballast layer, the embankment layer also shows an amplification of the strain energy for model-L3 in AZ-I. In AZ-II (Fig. 14b), model-L1 shows the most promising behaviour because of both the decreasing spatial trend and the (temporal) smoothness (no abrupt increase or decrease) of the strain energy. In AZ-III (Fig. 14c), however, all models result in similar strain energy curves.

Subgrade: Fig. 15 shows a comparison of the time histories of strain energy in the subgrade layer for zones AZ-I, AZ-II and AZ-III, for models L1-L5. No amplification of strain energy is observed for any of the longitudinal profiles under study in AZ-I (Fig. 15a). No spatial decreasing trend in the magnitude of the strain energy is observed for models L2 and L4 from AZ-I to AZ-II (Fig. 15b). Models L1, L3 and L5 show a reduction in the magnitude of strain energy in AZ-II compared to that in AZ-I. However, model-L3 shows an abrupt decrease in the magnitude of strain energy in AZ-II compared to AZ-I. In the end, within zone AZ-II and AZ-III, all longitudinal profiles satisfy the strain energy criterion in terms of both spatial decreasing trend and smoothness.

Transverse profiles of SHIELD

Ballast: Fig. 16 shows a comparison of the time history of strain energy in the ballast layer for zones AZ-I (a), AZ-II (b) and AZ-III (c) for models T1-T4. In AZ-I, all the models illustrate the same strain energy distribution (no abrupt increase or decrease). In AZ-II, models T1 and T2

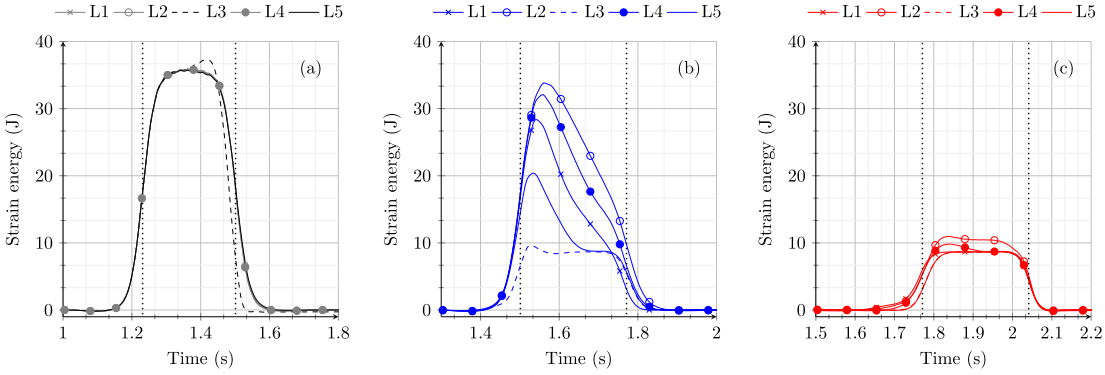

Fig. 14. Time history of strain energy for different longitudinal profiles under study in the layer of the embankment for (a) AZ-I, (b) AZ-II and (c) AZ-III. The dotted lines mark the time moments at which the load enters and exits each zone.

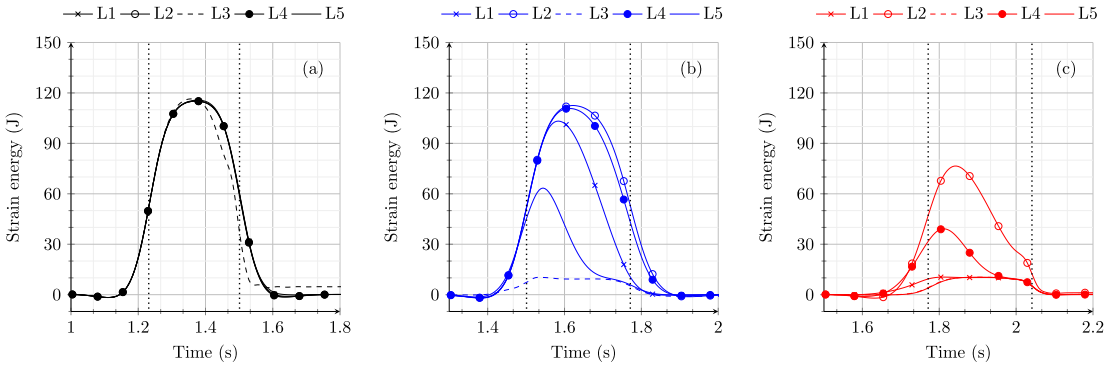

Fig. 15. Time history of strain energy for different longitudinal profiles under study in the layer of subgrade for (a) AZ-I, (b) AZ-II and (c) AZ-III. The dotted lines mark the time moments at which the load enters and exits each zone.

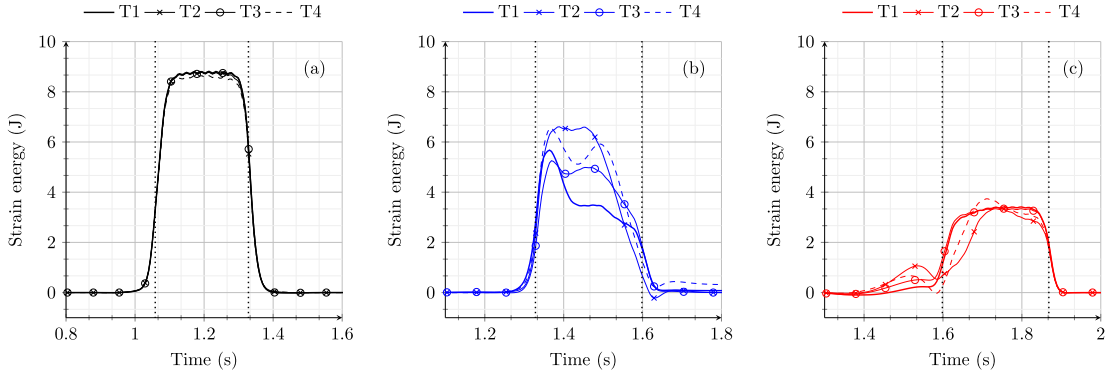

Fig. 16. Time history of strain energy for different transverse profiles under study in the layer of ballast for (a) AZ-I, (b) AZ-II and (c) AZ-III. The dotted lines mark the time moments at which the load enters and exits each zone.

show the most smooth distribution of strain energy demonstrating a gradual decrease in the magnitude of strain energy as the load approaches AZ-III (i.e., spatial trend). However, models T3 and T4 show a non-smooth (similar to Fig. 10d) temporal trend of strain energy in AZ-II, which can be associated with the geometric profiles of these models guiding or reflecting (see Introduction) energy towards the ballast layer (similar to the case shown in [34]). In the end, model-T1 shows the smoothest strain energy distribution also for AZ-III, proving it to be the most efficient geometric profile of SHIELD in guiding the energy flow according to the criterion discussed in Section Outputs.

Embankment: Fig. 17 shows a comparison of the time history of strain energy in the embankment layer for zones AZ-I (a), AZ-II (b) and AZ-III (c), for models T1-T4. It can be clearly seen that models T1 and T3 show a similar distribution of strain energy in all three zones for the embankment layer. Models T2 and T4 exhibit a higher strain energy magnitude in AZ-II and a less smooth distribution of strain energy in AZ-III compared to models T1 and T3. Nevertheless, none of the models show an amplification of strain energy in any of the zones under study.

Subgrade: Fig. 18 shows a comparison of the time history of strain energy in the subgrade layer for zones AZ-I, AZ-II and AZ-III, for models T1-T4. In AZ-I (Fig. 18 and AZ-II (Fig. 18b), all models show similar strain energy distributions. In AZ-III (Fig. 18c), models T1 and T3 show a very similar strain energy distribution and models T2 and T4 show a non-smooth strain energy distribution compared to the other models due to the higher magnitude of strain energy at the time moment when the load enters this zone. In the end, models T1 and T3 demonstrate the most efficient distribution of strain energy in the subgrade layer.

Vertical profiles of SHIELD

The time history of the strain energy is compared for two vertical profiles of the shield (models V1 and V2) for the layers of ballast

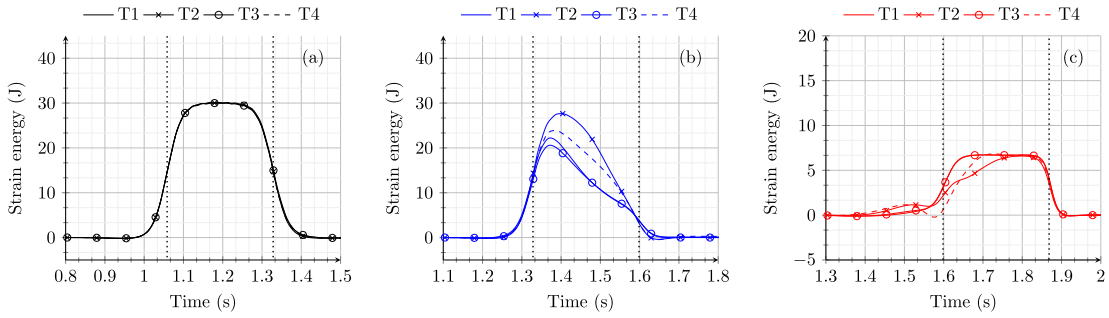

Fig. 17. Time history of strain energy for different transverse profiles under study in the layer of the embankment for (a) AZ-I, (b) AZ-II and (c) AZ-III. The dotted lines mark the time moments at which the load enters and exits each zone.

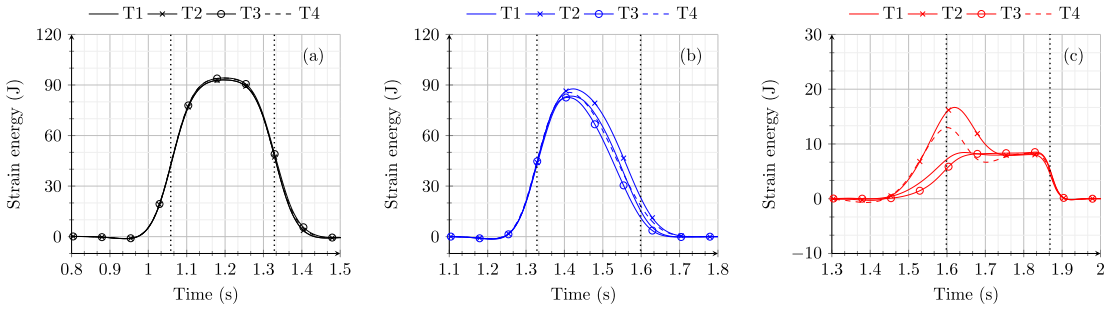

Fig. 18. Time history of strain energy for different transverse profiles under study in the layer of ballast for (a) AZ-I, (b) AZ-II and (c) AZ-III. The dotted lines mark the time moments at which the load enters and exits each zone.

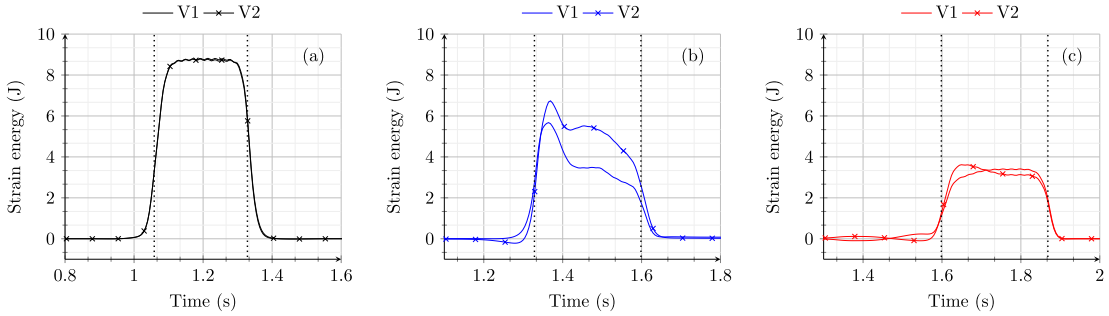

Fig. 19. Time history of strain energy for different vertical profiles under study in the layer of ballast for (a) AZ-I, (b) AZ-II and (c) AZ-III. The dotted lines mark the time moments at which the load enters and exits each zone.

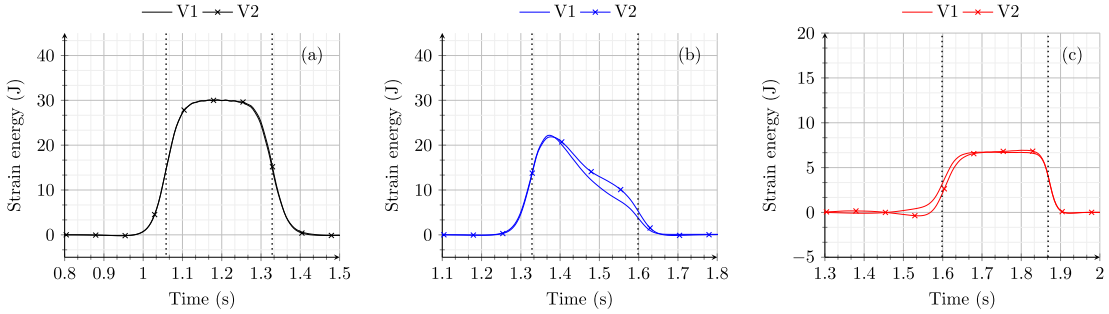

Fig. 20. Time history of strain energy for different vertical profiles under study in the layer of embankment for (a) AZ-I, (b) AZ-II and (c) AZ-III. The dotted lines mark the time moments at which the load enters and exits each zone.

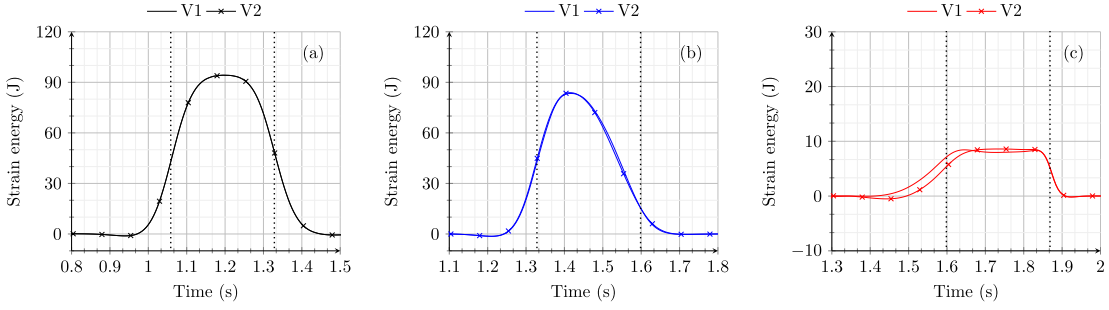

Fig. 21. Time history of strain energy for different vertical profiles under study in the layer of subgrade for (a) AZ-I, (b) AZ-II and (c) AZ-III. The dotted lines mark the time moments at which the load enters and exits each zone.

(Fig. 19), embankment (Fig. 20) and subgrade (Fig. 21). For the layers of embankment and subgrade, both profiles show nearly the same strain energy distribution for each of the zones under study. In the ballast layer, both models have the same energy distribution in AZ-I, model-V2 shows higher magnitudes of strain energy in AZ-II compared to model-V1 but shows a smoother decreasing temporal trend in AZ-III compared to model-V1. This concludes that the vertical cross-section of the shield at the interface with the concrete bridge can be tuned to achieve a decreasing temporal trend of strain energy in the proximity of the concrete structure (AZ-III). In the end, models V1 and V2 both satisfy

the criterion discussed in Section Outputs in terms of both spatial and temporal trends. However, the final choice will depend on other factors such as type of transition, speed of vehicle etc. For the set of parameters chosen in this work, model-V1 outperforms V2 in terms of the smoothness of the temporal trend in AZ-II.

Summary of results

The results in the preceding section show the influence of geometry in the three principle planes (longitudinal, transverse and vertical) in redistributing energy in railway transition zones. The energy is directly correlated to permanent deformations in the vicinity of the transition interface and the non-uniformity of energy distribution is correlated to non-uniform permanent deformations. In summary, on one hand, this analysis concludes that model-L1 has the most promising longitudinal geometric profile that aids an efficient redistribution of strain energy in all the zones under study and for all the trackbed layers (ballast, embankment and subgrade) according to the two-point evaluation criteria (spatial and temporal) discussed in Section Outputs. Moreover, considering the performance of all the transverse profiles studied in the previous section, model-T1 shows the optimum distribution of the strain energy in each of the trackbed layers (ballast, embankment and subgrade) according to the evaluation criteria. Therefore, the transverse profile of model-T1 is chosen as a starting point for the analysis of the influence of vertical profiles of SHIELD. In the end, when analysing vertical profiles, both models V1 and V2 satisfy the evaluation criteria in terms of both spatial and temporal trends. However, fine-tuning the vertical profiles can lead to a further smoothening of the temporal variation of strain energy curves in the vicinity of the transition interface. The current literature focuses only on longitudinal cross-sectional studies to minimise the degradation in railway transition zones. This work employs a novel energy-based criterion to highlight the need for the geometric optimisation of the transition structure in all geometric planes. Specifically, the role of optimising the transverse geometric profiles in energy redistribution was established through this work.

Conclusions

In this work, the effect of geometry on the spatial and temporal distribution of strain energy is studied for a standard embankment-bridge transition with and without a transition structure (SHIELD). The geometry of SHIELD is varied in longitudinal, transversal and vertical planes to investigate its influence on the redistribution of strain energy in the railway transition zones. In general, it is observed that the various zones and the trackbed layers of the railway transition zones react differently to different geometric profiles of SHIELD in terms of strain energy variations.

The ballast, embankment and subgrade layers demonstrate the highest sensitivity to the variation of the longitudinal profile of SHIELD compared to variations on the transverse and vertical profiles. The transverse profiles affect the ballast layer the most and optimising the vertical profile leads to a better distribution of strain energy in the zone next to the transition interface with the concrete structure. In the end, geometries in all directions (longitudinal, transverse and vertical) proved to be influential in one way or another in redistributing the energy flow in the RTZs. For the parameters (speed, trackbed material properties and type of transition) considered in this work, model-V1 proved to be the most efficient geometrical shape (in all directions) of SHIELD according to the strain energy criterion that associates the strain energy distribution to the operation-driven degradation. Even though the geometric shape of SHIELD suggested in this work might not be optimal for all types of site conditions (as the best-suited profile will depend on the above-mentioned parameters), it definitely highlights the importance of geometry in tuning the spatial and temporal strain energy distributions. This study is a preliminary investigation that aims to guide the designers in optimising the geometric profiles of transition structures for their specific requirements (specific type of transition zones and/or site conditions) aimed at uninterrupted energy flow in RTZs.

In conclusion, the research substantiates that optimizing the geometric profiles of SHIELD in all directions is vital in redistributing strain energy effectively, thereby reducing operation-driven degradation and extending the lifespan of RTZs. This study not only reinforces the shift towards an energy-centric design of RTZs but also has practical implications for design and maintenance. This paper suggests that by fine-tuning geometric profiles, we can significantly improve the performance and durability of the transition structures. The insights developed in this work pave the way for robust, energy-efficient and resilient design solutions using geometry as a tool, establishing the stepping stone for an exploration into the intricate relationship between geometry, strain energy and the performance of railway transition zones subjected to operation-driven settlement. It is to be noted that for an effective implementation, the optimised geometric design will be verified for critical conditions arising due to track irregularities, impact wheel loading, and train-track interactions in future works concerning SHIELD.

Declaration of Competing Interest

The authors declare that they have no known competing financial interests or personal relationships that could have appeared to influence the work reported in this paper.

Data availability

Data will be made available on request.

Acknowledgements

This research is supported by the Dutch Technology Foundation TTW (Project 15968), a part of the Netherlands Organisation for Scientific Research (NWO), and which is partly funded by the Ministry of Economic Affairs.

References

[1] Fortunato E, Paixão A, Calçada R. Railway track transition zones: design, construction, monitoring and numerical modelling. Int J Railway Technol 2013;2(4):33–58. https://doi.org/10.4203/ijrt.2.4.3.
[2] Design of Track Transitions, Transportation Research Board, 2006. https://doi.org/10.17226/23228.
[3] Namura A, Suzuki T. Evaluation of countermeasures against differential settlement at track transitions. Quart Rep RTRI 2007;48(3):176–82. https://doi.org/10.2219/rtriqr.48.176.
[4] Coelho B, Hölscher P, Priest J, Powrie W, Barends F. An assessment of transition zone performance. Proc Inst Mech Eng, Part F: J Rail Rapid Transit 2011;225(2):129–39. https://doi.org/10.1177/09544097JRRT389.
[5] Indraratna B, Sajjad MB, Ngo T, Correia AG, Kelly R. Improved performance of ballasted tracks at transition zones: a review of experimental and modelling approaches. Transport Geotech 2019;21:100260. https://doi.org/10.1016/j.trgeo.2019.100260.
[6] Sañudo R, dell'Olio L, Casado J, Carrascal I, Diego S. Track transitions in railways: A review. Constr Build Mater 2016;112:140–57. https://doi.org/10.1016/j.conbuildmat.2016.02.084.
[7] Metrikine A, Wolfert A, Dieterman H. Transition radiation in an elastically supported string. abrupt and smooth variations of the support stiffness. Wave Motion 1998;27(4):291–305. https://doi.org/10.1016/S0165-2125(97)00055-3.
[8] H.E.M. a. HUNT, Settlement of railway track near bridge abutments. (third paper in young railway engineer of the year (1996) award), Proceedings of the Institution of Civil Engineers - Transport 123 (1) (1997) 68–73. https://doi.org/10.1680/itran.1997.29182.
[9] Stark TD, Wilk ST. Root cause of differential movement at bridge transition zones. Proc Inst Mech Eng, Part F: J Rail Rapid Transit 2015;230(4):1257–69. https://doi.org/10.1177/0954409715589620.
[10] Nielsen JC, Berggren EG, Hammar A, Jansson F, Bolmsvik R. Degradation of railway track geometry – correlation between track stiffness gradient and differential settlement. Proc Inst Mech Eng, Part F: J Rail Rapid Transit 2018;234(1):108–19. https://doi.org/10.1177/0954409718819581.
[11] Jain A, Metrikine A, Steenbergen M, Dalen K. Design of railway transition zones: a novel energy-based criterion. Transport Geotech 2024:101223. https://doi.org/10.1016/j.trgeo.2024.101223.

[12] Ognibene G, Powrie W, Pen LL, Harkness J. Analysis of a bridge approach: long-term behaviour from short-term response. In: 15th Railway Engineering Conference, Edinburgh, U.K.; 2019. p. 1–15.
[13] Sakhare A, Farooq H, Nimbalkar S, Dodagoudar GR. Dynamic behavior of the transition zone of an integral abutment bridge. Sustainability 2022;14(7):4118. https://doi.org/10.3390/su14074118.
[14] Ramos RCA, Gomes Correia A, Costa PA. Stress and permanent deformation amplification factors in subgrade induced by dynamic mechanisms in track structures. International Journal of Rail Transportation 2022;10(3):298–330. https://doi.org/10.1080/23248378.2021.1922317.
[15] Ramos A, Correia AG, Costa PA, Calçada R. Influence of track irregularities in the stress levels of the ballasted and ballastless tracks. In: Tutumluer E, Chen X, Xiao Y, editors. Advances in Environmental Vibration and Transportation Geodynamics. Singapore: Springer Singapore; 2020. p. 601–12.
[16] Varandas J, Hölscher P, Silva M. Three-dimensional track-ballast interaction model for the study of a culvert transition. Soil Dynam Earthquake Eng 2016;89:116–27. https://doi.org/10.1016/j.soildyn.2016.07.013.
[17] Shan Y, Albers B, Savidis SA. Influence of different transition zones on the dynamic response of track–subgrade systems. Comput Geotech 2013;48:21–8. https://doi.org/10.1016/j.compgeo.2012.09.006.
[18] Galvín P, Romero A, Domínguez J. Fully three-dimensional analysis of high-speed train–track–soil-structure dynamic interaction. J Sound Vib 2010;329(24):5147–63. https://doi.org/10.1016/j.jsv.2010.06.016.
[19] Banimahd M, Woodward PK, Kennedy J, Medero GM. Behaviour of train–track interaction in stiffness transitions. Proc Inst Civil Eng - Transp 2012;165(3):205–14. https://doi.org/10.1680/tran.10.00030.
[20] Laco K, Borzovič V. Reliability of approach slabs and modelling of transition zones of bridges. Appl Mech Mater 2016;821:741–6. https://doi.org/10.4028/www.scientific.net/amm.821.741.
[21] Heydari-Noghabi H, Zakeri J, Esmaeili M, Varandas J. Field study using additional rails and an approach slab as a transition zone from slab track to the ballasted track. Proc Inst Mech Eng, Part F: J Rail Rapid Transit 2017;232(4):970–8. https://doi.org/10.1177/0954409717708527.
[22] Coelho BZ, Hicks MA. Numerical analysis of railway transition zones in soft soil. Proc Inst Mech Eng, Part F: J Rail Rapid Transit 2015;230(6):1601–13. https://doi.org/10.1177/0954409715605864.
[23] Asghari K, Sotoudeh S, Zakeri J-A. Numerical evaluation of approach slab influence on transition zone behavior in high-speed railway track. Transportation Geotechnics 2021;28:100519. https://doi.org/10.1016/j.trgeo.2021.100519.
[24] Hu P, Zhang C, Wen S, Wang Y. Dynamic responses of high-speed railway transition zone with various subgrade fillings. Comput Geotech 2019;108:17–26. https://doi.org/10.1016/j.compgeo.2018.12.011.
[25] Paixão A, Fortunato E, Calçada R. A numerical study on the influence of backfill settlements in the train/track interaction at transition zones to railway bridges. Proc Inst Mech Eng, Part F: J Rail Rapid Transit 2015;230(3):866–78. https://doi.org/10.1177/0954409715573289.
[26] Paixão A, Fortunato E, Calçada R. Design and construction of backfills for railway track transition zones. Proc Inst Mech Eng, Part F: J Rail Rapid Transit 2013;229(1):58–70. https://doi.org/10.1177/0954409713499016.
[27] Palomo ML, Martínez JHA, Arnoa AZ, Medina JJC. Structural and vibration performance in different scenarios of a prefabricated wedge for railway transition zones. Journal of Vibration Engineering & Technologies 2021;9(7):1657–68. https://doi.org/10.1007/s42417-021-00319-5.
[28] Esmaeili M, Heydari-Noghabi H, Kamali M. Numerical investigation of railway transition zones stiffened with auxiliary rails. Proceedings of the Institution of Civil Engineers - Transport 2020;173(5):299–308. https://doi.org/10.1680/jtran.17.00035.
[29] Heydari-Noghabi H, Varandas JN, Esmaeili M, Zakeri J. Investigating the influence of auxiliary rails on dynamic behavior of railway transition zone by a 3d train-track interaction model. Latin Am J Solids Struct 2017;14(11):2000–18. https://doi.org/10.1590/1679-78253906.
[30] Jain A, Metrikine AV, Steenbergen MJMM, van Dalen KN. Dynamic amplifications in railway transition zones: performance evaluation of sleeper configurations using energy criterion. Frontiers in Built Environment 10. https://doi.org/10.3389/fbuil.2024.1285131.
[31] Ribeiro CA, Paixão A, Fortunato E, Calçada R. Under sleeper pads in transition zones at railway underpasses: numerical modelling and experimental validation. Structure and Infrastructure Engineering 2015;11(11):1432–49. https://doi.org/10.1080/15732479.2014.970203.
[32] Bizjak KF, Knez F, Lenart S, Slanc K. Life-cycle assessment and repair of the railway transition zones of an existing bridge using geocomposite materials. Structure and Infrastructure Engineering 2017;13(3):331–44. https://doi.org/10.1080/15732479.2016.1158288.
[33] Jia W, Markine V, Carvalho M, Connolly DP, Guo Y. Design of a concept wedge-shaped self-levelling railway sleeper. Constr Build Mater 2023;386:131524. https://doi.org/10.1016/j.conbuildmat.2023.131524.
[34] Jain A, Metrikine A, Steenbergen M, van Dalen K. Railway transition zones: evaluation of existing transition structures and a newly proposed transition structure. International Journal of Rail Transportation 2023:1–21. https://doi.org/10.1080/23248378.2023.2272668.
[35] K.N. van Dalen, A.V. Metrikine, Transition radiation of elastic waves at the interface of two elastic half-planes, Journal of Sound and Vibration 310 (3) (2008) 702–717, EUROMECH Colloquium 484 on Wave Mechanics and Stability of Long Flexible Structures Subject to Moving Loads and Flows. https://doi.org/10.1016/j.jsv.2007.06.007.
[36] van Dalen KN, Tsouvalas A, Metrikine AV, Hoving JS. Transition radiation excited by a surface load that moves over the interface of two elastic layers. Int J Solids Struct 2015;73–74:99–112. https://doi.org/10.1016/j.ijsolstr.2015.07.001.
[37] van Dalen KN, Steenbergen M. Modeling of train-induced transitional wavefields. In: Pombo J, editor. Proceedings of the 3rd international conference on railway technology. United Kingdom: Civil-Comp Press; 2016. p. 1–16. https://doi.org/10.4203/ccp.110.199.
[38] Jain A, van Dalen K, Steenbergen M, Metrikine A. Dynamic amplifications in railway transition zones: investigation of key phenomena. J Phys: Conf Ser 2024;2647(15):152002. https://doi.org/10.1088/1742-6596/2647/15/152002.
[39] Jain A, Marykovskiy Y, Metrikine AV, van Dalen KN. Quantifying the impact of stiffness distributions on the dynamic behaviour of railway transition zones. Transportation Geotechnics 2024;45:101211. https://doi.org/10.1016/j.trgeo.2024.101211.
[40] ABAQUS/Standard User's Manual, Version 6.9, Dassault Systèmes Simulia Corp, United States.
[41] Wang H, Markine V. Modelling of the long-term behaviour of transition zones: Prediction of track settlement. Eng Struct 2018;156:294–304. https://doi.org/10.1016/j.engstruct.2017.11.038.
[42] H. Wang, V. Markine, X. Liu, Experimental analysis of railway track settlement in transition zones, Proc Inst Mech Eng, Part F: J Rail Rapid Transit 232 (6) (2018) 1774–1789, pMID: 30662168. https://doi.org/10.1177/0954409717748789.
[43] Wang H, Markine V. Dynamic behaviour of the track in transitions zones considering the differential settlement. J Sound Vib 2019;459:114863. https://doi.org/10.1016/j.jsv.2019.114863.
[44] ABAQUS Online Documentation: Version 6.6-1, Dassault Systèmes Simulia Corp, United States.
[45] Jain A, van Dalen K, Metrikine A, Faragau A, Steenbergen M. Comparative analysis of the dynamic amplifications due to inhomogeneities at railway transition zones. In: J. Pombo (Ed.), Proceedings of The Fifth International Conference on Railway Technology: Research, Development and Maintenance, Vol. CCC 1 of Civil-Comp Conferences, Civil-Comp Press, United Kingdom; 2023. https://doi.org/10.4203/ccc.1.19.1.
[46] Jain A, Metrikine A, Steenbergen M, van Dalen K. Evaluation of a novel mitigation measure for two different types of railway transition zones. In: Proceedings of the Sixth International Conference on Railway Technology: Research, Development and Maintenance, Vol. 7 of RAILWAYS 2024, Civil-Comp Press, p. 1–11. https://doi.org/10.4203/ccc.7.17.1.